Tissue Eng Regen Med (2017) 14(3):317–326
DOI 10.1007/s13770-017-0032-7

Online ISSN 2212-5469
Print ISSN 1738-2696

ORIGINAL ARTICLE

Insights into the Therapeutic Potential of Heparinized Collagen Scaffolds Loading Human Umbilical Cord Mesenchymal Stem Cells and Nerve Growth Factor for the Repair of Recurrent Laryngeal Nerve Injury

Yongqin Pan[1] · Genlong Jiao[2] · Jingge Yang[1] · Rui Guo[3] · Jinyi Li[1] · Cunchuan Wang[1]

Received: 8 May 2016 / Revised: 5 July 2016 / Accepted: 22 August 2016 / Published online: 7 April 2017

Abstract Recurrent laryngeal nerve (RLN) injury can result in unilateral or bilateral vocal cords paralysis, thereby causing a series of complications, such as hoarseness and dyspnea. However, the repair of RLN remains a great challenge in current medicine. This study aimed to develop human umbilical mesenchymal stem cells (HuMSCs) and nerve growth factor (NGF)-loaded heparinized collagen scaffolds (HuMSCs/NGF HC-scaffolds) and evaluate their potential in the repair of RLN injury. HuMSCs/NGF HC-scaffolds were prepared through incorporating HuMSCs and NGF into heparinized collagen scaffolds that were prefabricated by freeze-drying in a template. The resulting scaffolds were characterized by FTIR, SEM, porosity, degradation *in vitro*, NGF release *in vitro* and bioactivity. A rabbit RLN injury model was constructed to appraise the performance of HuMSCs/NGF HC-scaffolds for nerve injury repair. Electrophysiology, histomorphology and diagnostic proteins expression for treated nerves were checked after application of various scaffolds. The results showed that the composite scaffolds with HuMSCs and NGF were rather helpful for the repair of broken RLN. The RLN treated with HuMSCs/NGF HC-scaffolds for 8 weeks produced a relatively normal electromyogram, and the levels of calcium-binding protein S100, neurofilament and AchE pertinent to nerve were found to be close to the normal ones but higher than those resulted from other scaffolds. Taken together, HuMSCs/NGF HC-scaffolds exhibited a high score on the nerve injury repair and may be valuable for the remedy of RLN injury.

Keywords Recurrent laryngeal nerve injury · Human umbilical cord mesenchymal stem cells · Nerve growth factor · Collagen scaffolds · Heparin

1 Introduction

Recurrent laryngeal nerve (RLN) injury represents a serious complication of thyroid surgery, which can lead to dysfunction of vocal cord and airway smooth muscles. As a result of RLN injury, such diseases make a great burden to the individual family or the society, to which a myriad of efforts have been devoted [1]. In clinical practice, surgeons often employ the techniques of end-to-end anastomosis and autogenous nerve transplantation to repair the injured nerves [2, 3]. Due to the deprivation of proliferation and differentiation for mature neurons, the prosthetic effect of nerve regeneration and function restoration are not yet satisfactory. It is now evoking a keen interest to develop more applicable approaches for the repair of RLN injury.

Yongqin Pan and Genlong Jiao have contributed equally to this work.

✉ Jinyi Li
tlijy@jnu.edu.cn

✉ Cunchuan Wang
twcc@jnu.edu.cn

[1] Department of General Surgery, First Affiliated Hospital of Jinan University, No. 613 West Huangpu Avenue, Guangzhou 510630, People's Republic of China

[2] Department of Orthopedics, First Affiliated Hospital of Jinan University, Guangzhou 510630, People's Republic of China

[3] College of Life Science and Technology, Jinan University, Guangzhou 510630, People's Republic of China

On the basis of microsurgery, tissue engineering has been receiving more attention for the repair of RLN injury. Tissue engineering refers to a combination strategy of cells, engineering and materials, and suitable biochemical factors to improve or repair the lost functions of the body [4]. A good scaffold should be provided with a biocompatible matrix with conduits, seed cells for tissue repair and nutritional factors for cell proliferation [5]. It has shown that collagen scaffold can promote the reinnervation when implanted into the site of the nerve lesion [6]. However, collagen as tissue engineering material possesses several shortcomings, such as low mechanical strength and fast degradation *in vivo*. To intensify the scaffolds, collagen is usually derived or used in combination with other materials [7–10]. Heparin is negatively charged that can firmly bind with most of proteins via intermolecular interaction [11]. The participation of heparin, for one thing, can enhance the mechanical strength of scaffolds, for another can facilitate loading of biochemical promoters. Heparinized collagen scaffolds may be more suitable for sustaining the payload release and assisting the proliferation of seed cell.

Aside from the scaffold, seed cell as well as its inducing factor plays an important role in never regeneration and repair. Stem cells are undifferentiated biological cells that can differentiate into specialized cells with characteristics of various tissues, such as muscles and nerves [12]. Depending on superior self-renewal ability and differentiation potential, a variety of cells have been applied in tissue engineering and cell transplantation therapy, including embryonic stem cells (ESCs), neural stem cells (NSCs), mesenchymal stem cells (MSCs), etc. Among these, human umbilical cord MSCs (HuMSCs) taken from the Wharton's Jelly tissue of newborn's umbilical cord are more primitive than adult MSCs, with stronger proliferation and self-renewal capacity [13]. HuMSCs have been shown able to differentiate into neural stem cells [14]. In most cases, nerve growth factor (NGF) is involved in stem cell-growing scaffolds for reinnervation so as to specifically induce them into nerve cells [15]. However, short half-life of NGF becomes a challenge for its use *in vivo*, which requires the scaffolds not only able to effectively load the seed cells, but also to achieve a sustained release of NGF. It is desirable to have biomimetic approach that can graft a bridge across the lesion while providing superior mechanical and biochemical supports for nerve regeneration through the axonal pathway [16]. Considering the abovementioned, it is hypothesized that heparinized collagen scaffolds (HC-scaffolds), as matrix of HuMSCs and NGF, have the capacity to enhance HuMSCs proliferation and control NGF release for nerve injury repair.

Stem cell therapy with the support of nerve scaffolds should be a promising strategy to cure the peripheral nerve injury. In this study, HuMSCs and NGF-loaded HC-scaffolds (HuMSCs/NGF HC-scaffolds) were engineered through co-culture of HuMSCs with NGF-loaded HC-scaffolds prefabricated by freeze-drying. HC-scaffolds were characterized by FTIR, SEM, porosity and *in vitro* degradation. The control ability of HC-scaffolds toward NGF release as well as their effects on cell proliferation was investigated. HuMSCs were then seeded into HC-scaffolds to form the composite scaffolds containing HuMSCs and NGF. Finally, a rabbit RLN injury model was constructed to evaluate the repair effect of HuMSCs/NGF HC-scaffolds on the anastomosed nerve.

2 Materials and methods

2.1 Materials

Collagen (type I from bovine tendon) was kindly provided by the Department of Biomedical Engineering of Jinan University. HuMSCs were obtained from Umbilical Cord Blood Stem Cell Bank of Guangdong Province. Heparin, collagenase I, N-hydroxysuccinimide ester (NHS), *N*-(3-dimethylaminopropyl)-*N*-ethylcarbodiimide hydrochloride (EDC), 4′,6-diamidino-2-phenylindole (DAPI) and 2-morpholinoethanesulfonic acid (MES) were purchased from Sigma-Aldrich (Shanghai, China). Recombinant Human β-NGF was purchased from UCallM Biotechnology (Wuxi, China). Penicillin-streptomycin solution, trypsin and all antibodies were provided by BD (Shanghai, China). Deionized water was produced by a Milli-Q water purifying system (Millipore, MA, USA). All other chemicals were of analytical grade and used as provided.

2.2 Fabrication of heparinized collagen scaffolds

Collagen powders were dispersed in 1% acetic acid solution and stirred for 24 h at ambient temperature to form a collagen solution (1%, w/v). Then, the solution was transferred into a 48-well plate and lyophilized for 48 h under −60 °C, in which porous collagen scaffolds (C-scaffolds) were produced. The heparinization of collagen scaffold followed a reported procedure with minor modification [17]. In brief, dry C-scaffolds were firstly immersed into 0.05 mg/mL MES buffer for 30 min, and then transferred into another MES buffer containing heparin (2 mg/mL), EDC (2 mg/mL) and NHS (1.2 mg/mL). The reaction was performed at 37 °C and maintained for 4 h. To remove the unreacted species, the scaffolds were soaked in 0.1 M Na_2HPO_4 solution for 2 h and then rinsed three times with deionized water. Finally, the heparinized collagen scaffolds (HC-scaffolds) were harvested via freeze-drying under −60 °C again.

2.3 Characterization of HC-scaffolds

2.3.1 FTIR

Aliquots of heparin, C-scaffolds and HC-scaffolds (~2 mg) were prepared into infrared transparent matrixes with KBr. FTIR-8400S spectrometer (Shimadzu, Toyota, JPN) was used to scan the samples. FTIR spectra were recorded from 4000 cm^{-1} to 500 cm^{-1} with a resolution of 1 cm^{-1}.

2.3.2 SEM

Lyophilized C-scaffolds and HC-scaffolds were fixed to the supporter of SEM probe with double-sided tape. The samples were sputtered with gold-palladium and then subjected to SEM scanning (ZEISS EVO MA, Oberkochen, Germany). Micrographs were collected at a voltage of 5 kV.

2.3.3 Porosity analysis

Porosity measurement of scaffolds referred to the literature [18]. The sample was dried at 45 °C for 1 d and weighted (W_s). Then, the sample was put into a pycnometer filled with ethanol (totally weighted as W_1). The pycnometer was subsequently placed into a vacuum container to degas the sample, thus pushing ethanol into the space occupied by the air. The fluid surface in the pycnometer fell down due to back filling of ethanol. After degassing, the pycnometer was filled up with ethanol to the initial level. The weight of the pycnometer at this time was designated as W_2. Afterwards, the sample was took out and weighted the pycnometer as W_3. The porosity (ε) can be calculated according to the equation below:

$$\varepsilon = \frac{W2 - W3 - Ws}{W1 - W3} \times 100\%$$

2.3.4 In vitro degradation test

Degradation of various scaffolds was investigated in the collagenase I solution (0.01 M PBS, pH 7.4) [19]. In brief, a certain amount of scaffolds (0.5 g) were dispersed in 100 mL of blank PBS, 0.1 and 1 UI/mL collagenase solution, respectively. The collagenase solution was renewed every day. At the time points of 1, 3, 5, 7 and 9 d, the scaffolds were withdrawn, dried to constant weight, and weighed. All experiments were performed in triplicate. The degradation rate of scaffolds was expressed as the lost mass relative to the initial mass of scaffolds.

2.4 Preparation of NGF-loaded scaffolds

To load NGF onto the scaffolds, NGF solution was introduced into the wells of the plate containing dry HC-scaffolds where each well was added 100 ng of NGF. Then, the scaffolds adsorbing NGF were placed in the refrigerator of 4 °C overnight. Following adsorption of NGF, the scaffolds were lyophilized through the process mentioned above and NGF-loaded scaffolds were obtained after 48 h. In this study, both NGF-loaded C-scaffolds (as a control) and HC-scaffolds were prepared.

2.5 *In vitro* release of NGF from scaffolds

In vitro release of NGF from scaffolds was performed in pH 7.4 PBS. An aliquot of scaffolds (20 mg) was put into a flask containing 10 mL of PBS. The flask was then placed in a thermostatic oscillator. The release started at 37 °C with a vibration frequency of 100 times/min. At predetermined time intervals, 0.2 mL of solution was retrieved and replaced by the same volume of fresh PBS. The concentration of NGF in the release medium was determined using human β-NGF ELISA kit (R&D Systems, MN, USA) according to the product instruction. The total NGF in the scaffolds was quantified based on the same method by directly dissolving scaffolds in 1% acetic acid solution.

2.6 Effects of scaffolds on cell viability

The scaffolds were placed in a 96-well plate in which Dulbecco's modified Eagle's medium (DMEM) was introduced (0.1 mL/well). HuMSCs were seeded in the scaffold-containing plate with a density of 5×10^3/well. After culturing overnight, the culture medium was replaced every other day. Cell viability of HuMSCs in the presence of NGF-loaded C-scaffolds or HC-scaffolds was measured at the day of 1, 3, 5 and 7 by Cell Counting Kit-8 (CCK8) assay [20].

2.7 Therapeutic evaluation of HuMSCs/NGF HC-scaffolds on RLN injury

2.7.1 Preparation of HuMSCs/NGF HC-scaffolds

HuMSCs of passage 4 were used to construct HuMSCs/NGF HC-scaffolds. In brief, 0.25 mL of HuMSCs (1×10^6 cells/mL) was added into a 48-well plate loading sterile NGF-loaded HC-scaffolds. The wells were then supplemented with culture medium to submerge the surface of scaffolds. HuMSCs-laden scaffolds were maintained in the cell culture incubator for 12 h at 37 °C with 5% CO_2. The resulting HuMSCs/NGF scaffolds were used for the study of RLN injury repair. Likewise, HuMSCs HC-scaffolds, as a control, were prepared based on the same procedure using HC-scaffolds with no NGF.

2.7.2 Surgery and treatment

New Zealand rabbits were fasted for 8 h, but allowed free access to water before surgery. To anaesthetize the rabbits,

3% pentobarbital sodium solution was injected into the rabbits through the ear vein with a dose of 30 mg/kg. After skin preparation and disinfection, an incision was made on the throat to expose RLN. At the right side of 3 cm from the cricothyroid joint, the RLN was cut off and the epineurium was anastomosed by end-to-end. The animal experiment was approved by the Experimental Animal Ethical Committee of Jinan University (Approval No: SCXK 2011-0015).

Experimental rabbits were randomly divided into five groups ($n = 12$) that were implanted with nothing, C-scaffolds, HC-scaffolds, HuMSCs HC-scaffolds and HuMSCs/NGF HC-scaffolds, respectively. In detail, an appropriate amount of scaffold materials was fixated around the anastomosis site to form a 5 mm length of circumvolutio. The RLN was marked with a blue line after treatment. Then, the incision was sutured and sterilized. A sham-operated group that rabbits' RLN were preserved intact was done as a control. To prevent infection, the rabbits were intravenously injected with penicillin (30,000 UI/kg) and 5% glucose every day until the fifth day after operation. Experimental rabbits were taken care for 8 weeks, and physiological and pathological examinations were performed on the 4th and 8th week, respectively.

2.7.3 Electrophysiological examination

After 4 weeks and 8 weeks of treatment, the rabbits were anaesthetized as described above and a surgical incision was made at the same position in the previous operation. Before surgery, the rabbits were fasted for 8 h. The surrounding tissues of RLN were carefully isolated under a microscope. By identifying the mark line, the RLNs that were treated with different scaffolds were located. The electromyogram of RLN was detected using an EMG device (Trigno mobil, Delsys, Inc., MA, USA). The current intensity for stimulation was 0.07 MA. The exciting electrode was put on the position of RLN 4 cm from the throat and the reference electrode was inserted into the subcutaneous tissue in front of the sternum.

2.7.4 Histomorphological examination

Hematoxylin and eosin (H.E.) staining and immunohistochemical analysis were utilized to examine the histological changes of repaired RLNs. After electromyography detection, a length of RLN ($\sim$1 cm) distal to the anastomotic site was cut off. The nervous tissues were fixated with 4% paraformaldehyde and then prepared into paraffin sections for H.E. staining. After staining with H.E., the histomorphology of nerves was observed and recorded by a CX31 microscope (Olympus, Tokyo, Japan). Other paraffin sections proceeded to be used for immunohistochemical analysis for calcium-binding protein S100, neurofilament (NF) and acetylcholine enzyme (AchE) using anti-S100 (1:500), anti-NF (1:1000) and anti-AchE (1:200) antibodies (Abcam, Cambridge, UK). Goat anti-rabbit IgG-HRP was applied as a secondary antibody (1:1000) with 3,3'-diaminobenzidine (DAB) as a color-developing agent.

2.7.5 Western blotting

The obtained nerve tissues were cut into pieces and digested with 0.15% collagenase II. The cell suspensions were centrifuged for 5 min at 5000 rpm to collect cell pellets. Then, the lysates were prepared by lysing cells with radio immunoprecipitation assay (RIPA) lysis buffer (Beyotime, Shanghai, China) for 30 min on ice. The lysates were centrifuged at 15,000 rpm for 10 min in which the protein concentration was quantified by bicinchoninic acid (BCA) assay. Samples with equal protein level were loaded onto SDS-PAGE electrophoresis gel. After electrophoresis, the protein was transferred to a PVDF membrane (Haoran Biotech, Shanghai, China). The membrane was firstly blocked with 5% fat-free milk for 1 h at room temperature and then incubated with antibodies against S100, NF and AchE overnight at 4 °C. After that, the membranes continued to incubate with goat anti-rabbit IgG-HRP for 1 h at 37 °C. The membranes were further rinsed with PBS and counterstained with DAPI (10 μg/ml in PBS) followed by the detection of electrochemiluminescence (ECL) using a microscope (CKX41, Olympus, Tokyo, Japan) [21]. Band intensities were measured by densitometry using the Quantity One software with β-actin as a control.

3 Results and discussion

3.1 Fabrication and texture of HC-scaffolds

C-scaffolds were easily achieved through the process of lyophilization. To render the scaffolds heparin-functional, we employed a reaction of amidation between the carboxyl of heparin and the amino group of collagen to conjugate heparin onto collagen. The conjugation took place on the surface of C-scaffolds, which preserved both the porous texture of scaffolds and the function of heparin. FTIR confirmed that HC-scaffolds have been successfully fabricated (Fig. 1). The characteristic peaks of C-scaffolds located at 1659 cm^{-1}, 1552 cm^{-1}, 1461 cm^{-1}, 1249 cm^{-1} and 1254 cm^{-1} (Fig. 1A). Heparin displayed a similar FTIR spectrum to that of C-scaffolds, except for the position of 3345 cm^{-1} (Fig. 1B). The FTIR spectrum of HC-scaffolds resembled the one of C-scaffolds (Fig. 1C), but it comprised the characteristic peaks of heparin likewise, especially at 3345 cm^{-1}, 2998 cm^{-1} and 1552 cm^{-1} (as indicated by vertical lines). The results of FTIR provide information that heparin has been grafted onto the collagen matrix.

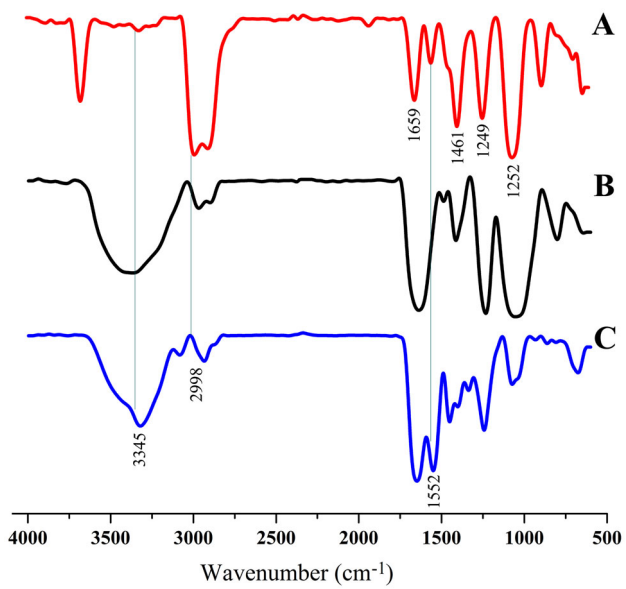

Fig. 1 FTIR spectra of collagen scaffolds **A**, heparin **B** and heparinized collagen scaffolds **C**

SEM revealed that C-scaffolds appeared to be a spongy matrix and there were considerable micropores existent (Fig. 2A). The pore size was approximately 150 ~ 200 μm as estimated from the scale bar. When heparinized, the morphology of scaffolds has changed obviously and accompanied with the reduction of pore size. HC-scaffolds seemed more compact and tougher compared with C-scaffolds (Fig. 2B). The pore size was reckoned to be 50 ~ 100 μm, significantly smaller than that of C-scaffolds. Also, this indicates that a crosslinking between heparin and C-scaffolds has actually occurred.

The porosity of C-scaffolds was measured to be 94.2 ± 1.9%, whereas it was 76.5 ± 4.5% for HC-scaffolds. The pore size and porosity of HC-scaffolds were both lower than those of C-scaffolds. It may be attributed to the collapse of porous architecture due to repeated soakage and lyophilization during the process of heparinization. Furthermore, the crosslinking between heparin and C-scaffolds also led to the decline of pore and porosity. However, it was noted that the porosity of HC-scaffolds was still above 70%, which was qualified for application in tissue engineering as 3D porous scaffold material [22].

Figure 3 shows the degradation profiles of C–scaffolds and HC-scaffolds in media with different level of collagenase. In blank PBS, two scaffolds exhibited low degradation within 9 days (cumulative degradation both less than 15%), demonstrating two scaffolds rather stable in the absence of collagenase. With the increase of collagenase concentration, the degradation of two scaffolds became fast, especially at the level of 1 UI/mL. However, there was a significant difference in degradation rate between C-scaffolds and HC-scaffolds. C-scaffolds were fully degraded within 5 days, but HC-scaffolds just degraded 20% around. Even on the 9th day, the cumulative degradation of HC-scaffolds was merely 36.7%. We assumed that this was because that the crosslinking between heparin and collagen built a barrier toward the approach of collagenase. In addition, smaller pore size and porosity significantly reduced the contact area of collagenase to HC-scaffolds, which further reduced the degradation down. These results indicate that HC-scaffolds not only are biodegradable in the presence of collagenase, but can protect the degradation from collagenase to some extent. The improved texture renders HC-scaffolds more suitable for RLN repair.

3.2 Preparation and characterization of NGF-loaded scaffolds

NGF possesses a high molecular mass that can result in stable entrapment into the micropores of scaffolds once

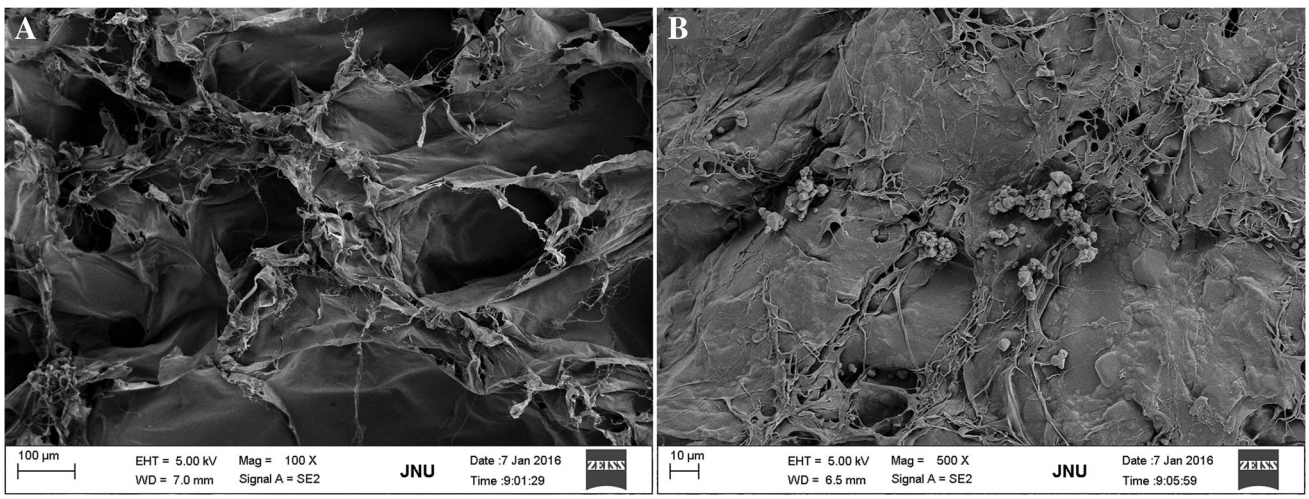

Fig. 2 TEM micrographs of collagen scaffolds **A** and heparinized collagen scaffolds **B**

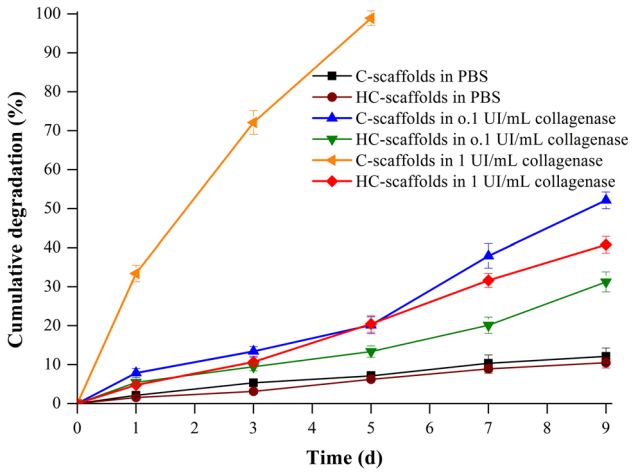

Fig. 3 *In vitro* degradation profiles of C-scaffolds and HC-scaffolds in PBS and collagenase solution of different concentration

precipitation. The loading process of NGF was quite straightforward and its biological activity was also maintained well. The heparin conjugated onto the scaffolds further facilitated the loading of NGF by way of heparin-protein interaction [11]. NGF release was also delayed through HC-scaffolds compared to C-scaffolds (Fig. 4). The release of NGF from C-scaffolds was rather rapid with a complete release on the 4th day. In the case of HC-scaffolds, the cumulative release was only 18.1% within 24 h. It spent 10 days to reach a full release of NGF. The participation of heparin allowed NGF to be immobilized electrostatically to the matrix due to charging oppositely [23]. Heparinization not only enhanced the mechanical strength of scaffolds, but also achieved a controlled release toward NGF.

Effects of NGF-loaded C-scaffolds and HC-scaffolds on HuMSCs proliferation are shown in Fig. 5. HuMSCs presented an incremental growth on the two scaffolds. There was no difference in cell proliferation between C-scaffolds and HC-scaffolds. They were both biocompatible with HuMSCs. The use of heparin did not affect the biocompatibility of scaffolds. The merit imparted NGF-loaded HC-scaffolds an excellent characteristic for application in tissue engineering.

3.3 Enhanced repair of RLN injury using HuMSCs/NGF HC-scaffold

After treating for 4 weeks, the rabbits' RLNs of all groups just produced some feeble action potential upon electric stimulation. Meanwhile, the waveforms were complicated and there was no significant difference in amplitude (peak-to-peak value) among groups (data not shown). After 8 weeks, RLNs from different model rabbits exhibited distinct responses of electrophysiology. Representative electromyograms of RLNs as well as the amplitudes of action potential are shown in Fig. 6. The groups treated with nothing or pure scaffolds brought about relatively low action potentials, and the latent times were also delayed (Fig. 6A, B, C). These results indicate that the broken nerves have been successfully joined, but the function of conduction has not been established. The groups treated with HuMSCs-accreted scaffolds exhibited augmentative action potentials, especially for the group of HuMSCs/NGF HC-scaffolds (Fig. 6D, E). The latent time became forward as well. The amplitude and latent time of electromyogram can be used to judge the recovery degree of injured nerves [24, 25]. It was evident that the participation of HuMSCs was helpful for the repair of RLN injury. By contrast, HuMSCs/NGF HC-scaffolds seemed to be more efficient in the nerve repair from the result of the electromyography.

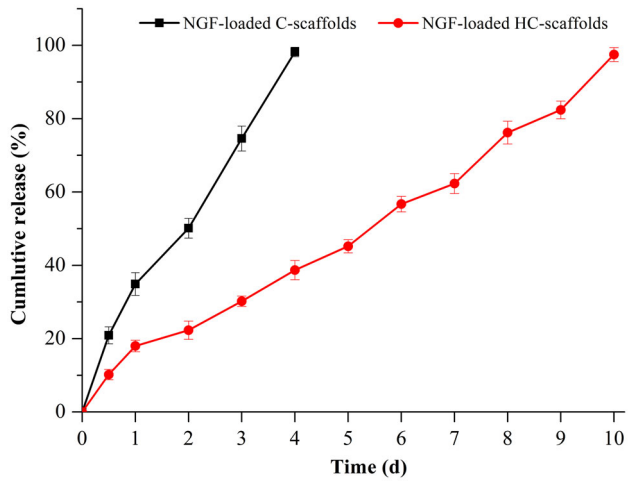

Fig. 4 Release profile of NGF from C-scaffolds and HC-scaffolds performed in pH 7.4 PBS (mean ± SD, $n = 3$)

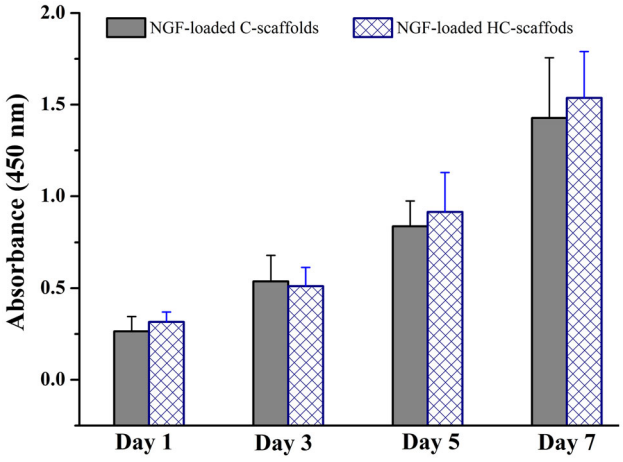

Fig. 5 HuMSCs cell viability as a function of culture time in the presence of NGF-loaded C-scaffolds or HC-scaffolds using CCK8 assay

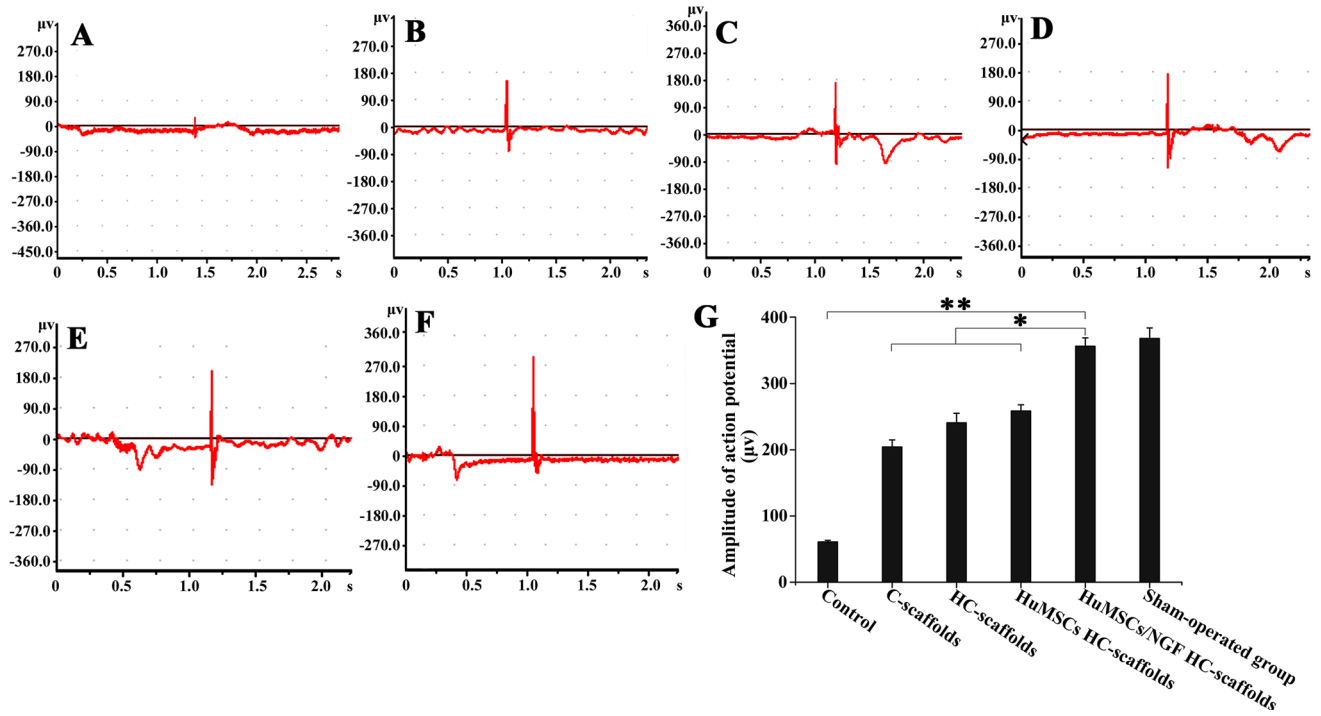

Fig. 6 Electromyograms of the RLNs after treatment for 8 weeks with nothing **A**, C-scaffolds **B**, HC-scaffolds **C**, HuMSCs HC-scaffolds **D** and HuMSCs/NGF HC-scaffolds **E**. Graph **F** is the electromyogram of sham-operated group and graph **G** represents the amplitudes (peak-to-peak value) of action potential of various groups (One-way ANVOA, $*p < 0.05$; $**p < 0.01$, significantly different between each other)

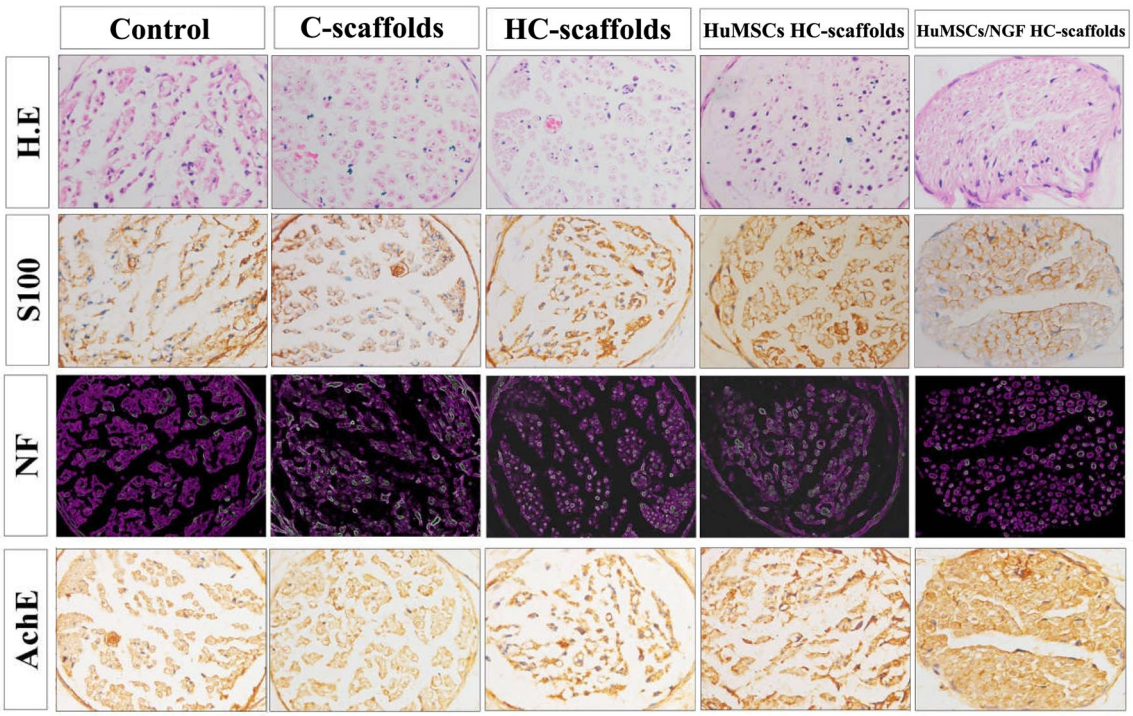

Fig. 7 Representative histological features of the RLN sections stained with HE and immunohistochemical results on S100, NF and AchE

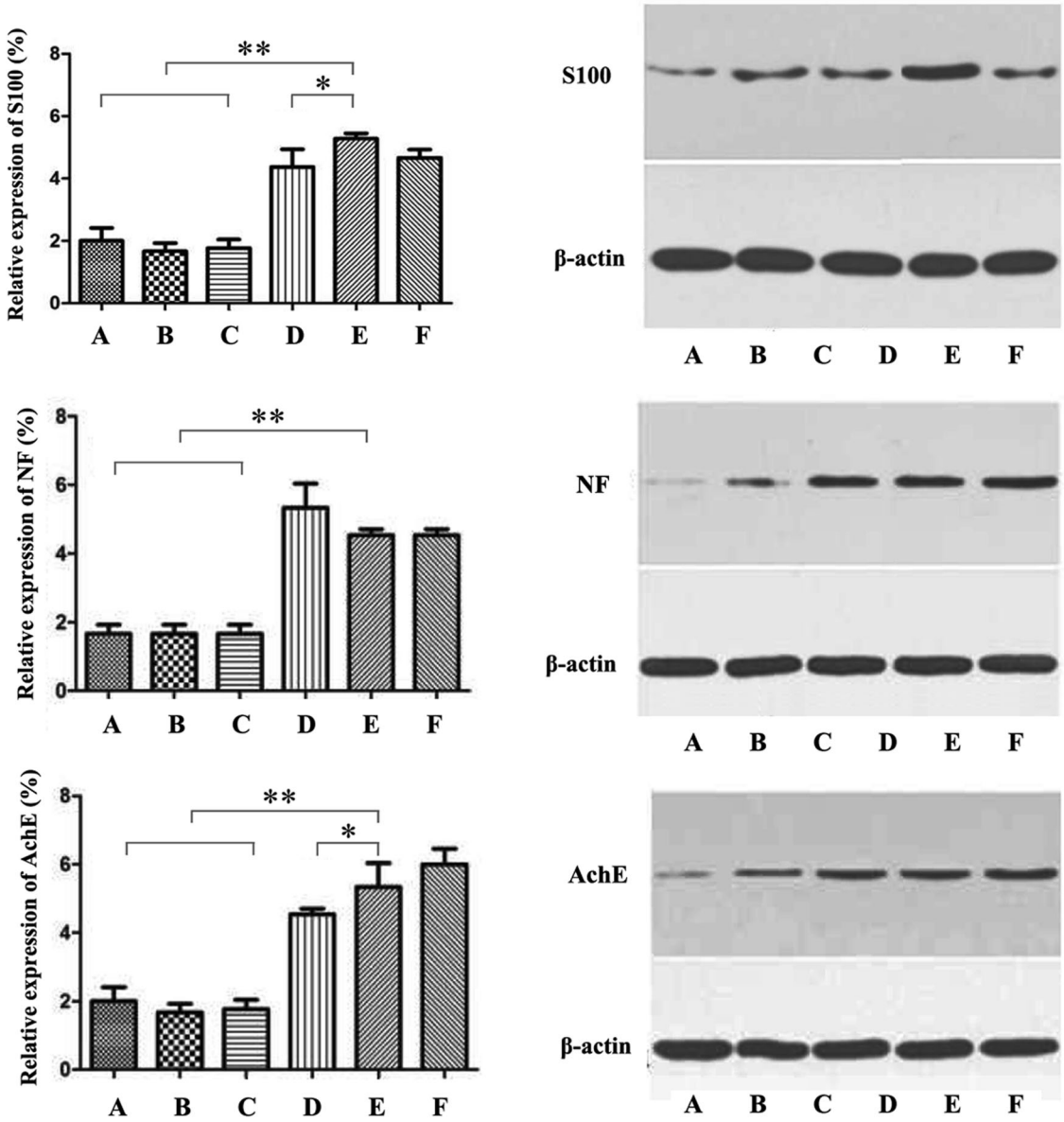

Fig. 8 Protein level of S100, NG and AchE in RLNs analyzed by western blotting: **A** Control, **B** C-scaffolds, **C** HC-scaffolds, **D** HuMSCs HC-scaffolds, **E** HuMSCs/NGF HC-scaffolds and **F** Sham-operated group (One-way ANVOA, $*p < 0.05$; $**p < 0.01$, significantly different between each other)

The electromyogram of HuMSCs/NGF HC-scaffolds group resembled that of sham-operated group in amplitude and latent time (Fig. 6F). NGF can drive the expression of genes such as Bcl-2 through binding to the TrkA receptor that stimulates the proliferation and survival of neurons [26]. It has been found that embryonic stem cells can migrate toward the nerve lesions and differentiate into neurons and astrocytes, thus repairing the RLN well [27]. HuMSCs are characterized by embryonic neural stem cells. Therefore, it is reasonable that HuMSCs/NGF HC-scaffolds will result in a better performance in the repair of RLN injury.

Histomorphology with H.E. staining and immunohistochemistry on S100, NF and AchE of resumptive RLNs after treatment for 8 weeks are shown in Fig. 7. For the control group, the distal fibers of the nerve's lacerated end disappeared. There were a large number of inflammatory cells infiltrating the nerve tissue. The group treated with C-scaffolds exhibited a reduced degree of inflammation in comparison with the control. HC-scaffolds posed a similar outcome to the lacerated nerve like C-scaffolds, other than a lighter inflammation. HuMSCs HC-scaffolds presented an enhanced repair effect on the lacerated nerve. The distal nerve fibers started to appear and the inflammatory cells

continued to reduce. Compared with other scaffolds, HuMSCs/NGF HC-scaffolds demonstrated a superior performance in the repair of RLN injury. After 8 weeks, most of the distal nerve fibers have recovered with the support of HuMSCs/NGF HC-scaffolds. It could be observed that there were clear nerve fibers arranged in order. The contribution of HuMSCs and NGF to the repair of RLN injury was affirmative.

Immunohistochemical results provided evidence that the composite scaffolds with HuMSCs and NGF were more suitable for the repair of RLN injury. The acidic calmodulin S100 relevant to the nervous tissue increased in sequence of control, C-scaffolds, HC-scaffolds, HuMSCs scaffolds and HuMSCs/NGF HC-scaffolds. Calmodulin S100 mainly exists in the astrocytes, which are characteristic star-shaped glial cells in the brain and spinal cord [28]. More calmodulin S100 expressing on RLNs treated with HuMSCs scaffolds betokens that HuMSCs have differentiated into nerve cells. It happens that there are similar cases for NF and AchE. NF chiefly consists of NF-1, NF-M and NF-H protein subunit that is always found in the mature neurocytes [29]. AchE plays a positive role in the growth and maturation of cells and can promote the development and regeneration of nerve cells [30]. High distribution within the nerve tissue of three mark proteins indicates that HuMSCs have developed into nerve cells to repair the injured nerve. Figure 8 displays the relative expression levels of S100, NF and AchE from Western blotting. The results were consistent with the immunohistochemical findings.

Conduit, sustentacular cell, neurotrophic factor and extracellular matrix are the basic elements of biomaterials for tissue engineering. Due to limitation of the body to regenerate axonal pathways, it is desirable to take advantage of a biomimetic approach that can bridge the lesion, while providing mechanical and biochemical supports for tissue regeneration. For instance, bone marrow stromal cells-seeded alginate hydrogel scaffolds have been used to promote axonal regeneration of injured RLN [31]. The alginate-based scaffolds with an anisotropic capillary structure physically guided the regeneration of axons. In another case, chitosan-derivative hydrogel scaffolds incorporating growth factors and neural stem/progenitor cells were developed to treat RLN injury [32]. The composite scaffolds resulted in a significant reduction in the lesion area and macrophage infiltration around the lesion site. Retrograde tracing and immunohistochemistry showed improvement of neuronal regeneration through the use of neural stem cells-laden scaffolds with growth factor. Our prepared HuMSCs/NGF HC-scaffolds are equipped with sustentacular cell, neurotrophic factor and 3D matrix with conduits. The results lend support to the speculation that incorporation of HuMSCs and NGF are able to further enhance the repair effect of collagen scaffolds on RLN injury compared with blank scaffolds.

In conclusion, the remedy for RLN injury represents a great challenge in clinical practice. This study engineered the composite scaffolds incorporating HuMSCs and NGF to bridge the broken nerve and evaluate its performance in RLN injury repair. HuMSCs/NGF HC-scaffolds were successfully prepared by embedding HuMSCs and NGF into the heparinized collagen scaffolds. The engineered scaffolds were acceptable in texture and control release of NGF. The suitability of HuMSCs/NGF HC-scaffolds as nerve repair material was verified by a RLN fracture model. Electrophysiological and histomorphological examinations as well as Western blotting assay demonstrated that HuMSCs/NGF HC-scaffolds were more applicable for the repair of nerve injury than those scaffolds with no HuMSCs and/or NGF. The results show that the composite scaffolds with HuMSCs and NGF are promising for the repair of RLN injury that occurs in the thyroid surgery.

Acknowledgements This work was supported by the Medical Science Fund Project of Guangdong Province, P.R. China (No. B2012192).

Compliance with ethical standards

Conflict of interest The authors declare that there are no any conflicts of interest.

Ethical statement All animal experiments were conducted according to the Guidelines on the Care and Use of Animals for Scientific Purposes (2004, Singapore). The animal experiment protocol was reviewed and approved by the Experimental Animal Ethical Committee of Jinan University (Approval No: SCXK 2011-0015) (Guangzhou, China).

References

1. Siebert JR, Eade AM, Osterhout DJ. Biomaterial approaches to enhancing neurorestoration after spinal cord injury: strategies for overcoming inherent biological obstacles. Biomed Res Int. 2015;2015:752572.
2. Ma J, Sui T, Zhu Y, Zhu A, Wei Z, Cao XJ. Micturition reflex arc reconstruction including sensory and motor nerves after spinal cord injury: urodynamic and electrophysiological responses. J Spinal Cord Med. 2011;34:510–7.
3. Zhang SC, Ma YH, Liu HR, Zhang XS, Pan YT, Zheng XD. Intradural lysis and peripheral nerve implantation for traumatic obsolete incomplete paralysis. Surg Technol Int. 2006;15:276–81.
4. He Y, Lu F. Development of synthetic and natural materials for tissue engineering applications using adipose stem cells. Stem Cells Int. 2016;2016:5786257.
5. Hsu SH, Kuo WC, Chen YT, Yen CT, Chen YF, Chen KS, et al. New nerve regeneration strategy combining laminin-coated chitosan conduits and stem cell therapy. Acta Biomater. 2013;9:6606–15.
6. Han S, Wang B, Jin W, Xiao Z, Li X, Ding W, et al. The linear-ordered collagen scaffold-BDNF complex significantly promotes

functional recovery after completely transected spinal cord injury in canine. Biomaterials. 2015;41:89–96.
7. Suzuki H, Araki K, Matsui T, Tomifuji M, Yamashita T, Kobayashi Y, et al. Value of a novel PGA-collagen tube on recurrent laryngeal nerve regeneration in a rat model. Laryngoscope. 2015;126:E233–9.
8. Li X, Han J, Zhao Y, Ding W, Wei J, Han S, et al. Functionalized collagen scaffold neutralizing the myelin-inhibitory molecules promoted neurites outgrowth in vitro and facilitated spinal cord regeneration in vivo. ACS Appl Mater Interfaces. 2015;7:13960–71.
9. Xu Y, Zhang Z, Chen X, Li R, Li D, Feng S. A silk fibroin/collagen nerve scaffold seeded with a co-culture of schwann cells and adipose-derived stem cells for sciatic nerve regeneration. PLoS ONE. 2016;11:e0147184.
10. Yan F, Yue W, Zhang YL, Mao GC, Gao K, Zuo ZX, et al. Chitosan-collagen porous scaffold and bone marrow mesenchymal stem cell transplantation for ischemic stroke. Neural Regen Res. 2015;10:1421–6.
11. Peysselon F, Ricard-Blum S. Heparin-protein interactions: from affinity and kinetics to biological roles. Application to an interaction network regulating angiogenesis. Matrix Biol. 2014;35:73–81.
12. Nishio M, Nakahara M, Yuo A, Saeki K. Human pluripotent stem cells: towards therapeutic development for the treatment of lifestyle diseases. World J Stem Cells. 2016;8:56–61.
13. Ren H, Sang Y, Zhang F, Liu Z, Qi N, Chen Y. Comparative analysis of human mesenchymal stem cells from umbilical cord, dental pulp, and menstrual blood as sources for cell therapy. Stem Cells Int. 2016;2016:3516574.
14. Chen S, Zhang W, Wang JM, Duan HT, Kong JH, Wang YX, et al. Differentiation of isolated human umbilical cord mesenchymal stem cells into neural stem cells. Int J Ophthalmol. 2016;9:41–7.
15. Petrova ES. Injured nerve regeneration using cell-based therapies: current challenges. Acta Naturae. 2015;7:38–47.
16. Tian L, Prabhakaran MP, Ramakrishna S. Strategies for regeneration of components of nervous system: scaffolds, cells and biomolecules. Regen Biomater. 2015;2:31–45.
17. Wu JM, Xu YY, Li ZH, Yuan XY, Wang PF, Zhang XZ, et al. Heparin-functionalized collagen matrices with controlled release of basic fibroblast growth factor. J Mater Sci Mater Med. 2011;22:107–14.
18. She H, Xiao X, Liu R. Preparation and characterization of polycaprolactone-chitosan composites for tissue engineering applications. J Mater Sci. 2007;42:8113–9.
19. Yao C, Roderfeld M, Rath T, Roeb E, Bernhagen J, Steffens G. The impact of proteinase-induced matrix degradation on the release of VEGF from heparinized collagen matrices. Biomaterials. 2006;27:1608–16.
20. Wang Y, Wu P, Lin R, Rong L, Xue Y, Fang Y. LncRNA NALT interaction with NOTCH1 promoted cell proliferation in pediatric t cell acute lymphoblastic leukemia. Sci Rep. 2015;5:13749.
21. Bishop E, Theophilus EH, Fearon IM. In vitro and clinical studies examining the expression of osteopontin in cigarette smoke-exposed endothelial cells and cigarette smokers. BMC Cardiovasc Disord. 2012;12:75.
22. Krishnamurithy G, Murali MR, Hamdi M, Abbas AA, Raghavendran HB, Kamarul T. Proliferation and osteogenic differentiation of mesenchymal stromal cells in a novel porous hydroxyapatite scaffold. Regen Med. 2015;10:579–90.
23. Sakiyama-Elbert SE, Hubbell JA. Development of fibrin derivatives for controlled release of heparin-binding growth factors. J Control Release. 2000;65:389–402.
24. Cherian A, Baheti NN, Iype T. Electrophysiological study in neuromuscular junction disorders. Ann Indian Acad Neurol. 2013;16:34–41.
25. Zheng X, Hong W, Tang Y, Ying T, Wu Z, Shang M, et al. Discovery of a new waveform for intraoperative monitoring of hemifacial spasms. Acta Neurochir (Wien). 2012;154:799–805.
26. Lee R, Kermani P, Teng KK, Hempstead BL. Regulation of cell survival by secreted proneurotrophins. Science. 2001;294:1945–8.
27. Sykova E, Jendelova P. In vivo tracking of stem cells in brain and spinal cord injury. Prog Brain Res. 2007;161:367–83.
28. Fiacco TA, Agulhon C, McCarthy KD. Sorting out astrocyte physiology from pharmacology. Annu Rev Pharmacol Toxicol. 2009;49:151–74.
29. Lohrke S, Brandstatter JH, Boycott BB, Peichl L. Expression of neurofilament proteins by horizontal cells in the rabbit retina varies with retinal location. J Neurocytol. 1995;24:283–300.
30. Massoulie J, Pezzementi L, Bon S, Krejci E, Vallette FM. Molecular and cellular biology of cholinesterases. Prog Neurobiol. 1993;41:31–91.
31. Gunther MI, Weidner N, Muller R, Blesch A. Cell-seeded alginate hydrogel scaffolds promote directed linear axonal regeneration in the injured rat spinal cord. Acta Biomater. 2015;27:140–50.
32. Li H, Ham TR, Neill N, Farrag M, Mohrman AE, Koenig AM, et al. A hydrogel bridge incorporating immobilized growth factors and neural stem/progenitor cells to treat spinal cord injury. Adv Healthc Mater. 2016;5:802–12.